MoS_2 Nanosheets for the Detoxification of Hg^{2+} in Living Cells

Shanshan Xing, Chunqiu Xia, Xinyi Liu, Liangqia Guo,* Fengfu Fu

Ministry of Education Key Laboratory for Analytical Science of Food Safety and Biology, Fujian Provincial Key Laboratory of Analysis and Detection Technology for Food Safety, College of Chemistry, Fuzhou University, Fuzhou 350116, China

*Corresponding authors, e-mail: lqguo@fzu.edu.cn

Experimental

Supporting Figures

UV-Vis absorption spectra were recorded on a Lambda 750 UV-Vis spectrophotometer. Dynamic light scattering data (DLS) were measured by a Malvern Zetasizer Nano-2s laser particle size and Zeta potential analyzer. X-ray diffraction (XRD) pattern was performed on a Rigaku Ultima-IV X-ray diffractometer in the range of 5−75° by using a Cu Kα radiation source (λ = 1.5418). Raman spectrum was measured by a Renishaw inVia Raman microscope. Transmission electron microscopic (TEM) images were collected by a Thermo Scientific Talos F200S G2 scanning/transmission electron microscope at an accelerated voltage of 200 kV. Atomic force microscopic (AFM) images were taken by a Bruker Nanoscope IIID scanning probe microscope. X-ray photoelectron spectroscopy (XPS) was measured by an ESCALAB 250 X-ray photoelectron spectrometer. Agilent 7500 inductively coupled plasma mass spectrometer (ICP-MS) was used to determine the concentration of Hg^{2+}. The absorbance for cytotoxicity assay was measured by a TECAN Spark multimode microplate reader.

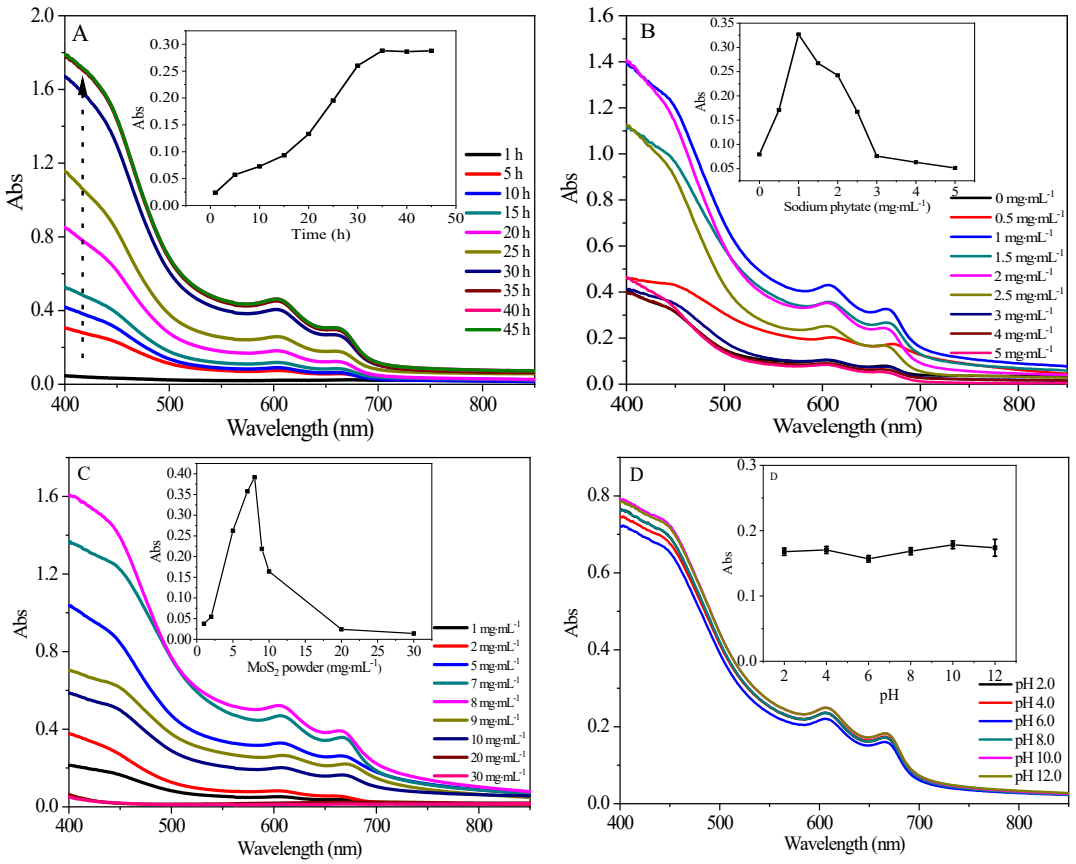

Figure S1. Absorption spectra of MoS_2 nanosheets exfoliated with different ultrasonic times (A), different concentrations of sodium phytate (B), different concentrations of MoS_2 powders (C); Absorption spectra of MoS_2 nanosheets (0.2 mg·mL^{-1}) dispersed in different pH phosphate buffer (10 mmol·L^{-1}) for three days (D). Insert of A, B and C is effect of ultrasonic time, concentration of sodium phytate, mass concentration of MoS_2 powder on the absorbance of MoS_2 nanosheets solution at 665 nm, respectively. Insert of D is the absorbance of MoS_2 nanosheets (0.2 mg·mL^{-1}) at 665 nm in different pH buffer. The pH was adjusted by 1.0 mol·L^{-1} HCl or NaOH solution.

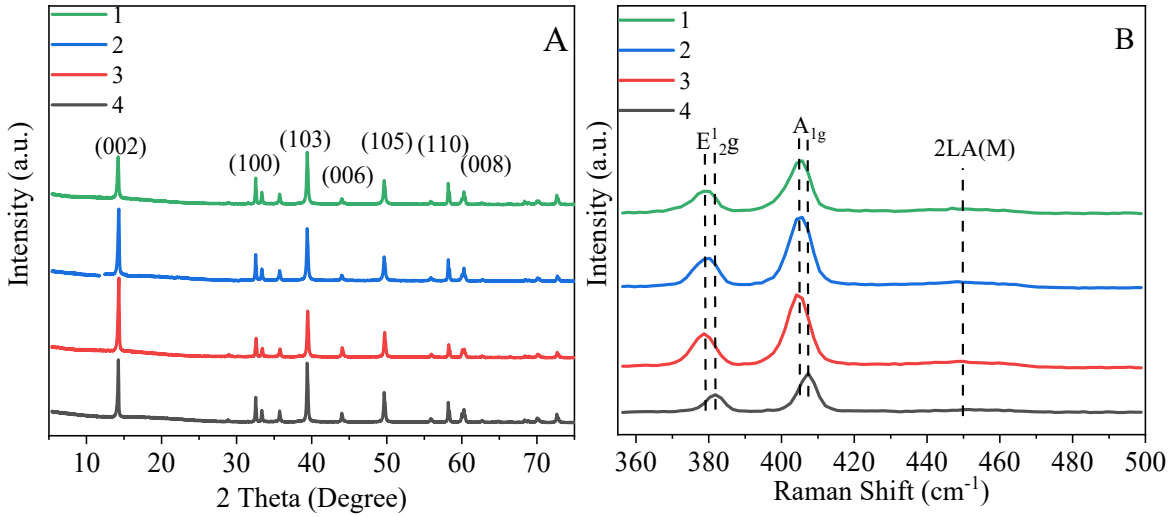

Figure S2. XRD patterns (A), and Raman spectra (B) of MoS_2 nanosheets exfoliated by sodium phytate (1), MoS_2 nanosheets exfoliated by Na_2HPO_4 (2), MoS_2 nanosheets exfoliated by H_2O (3), and bulk MoS_2 powder (4).

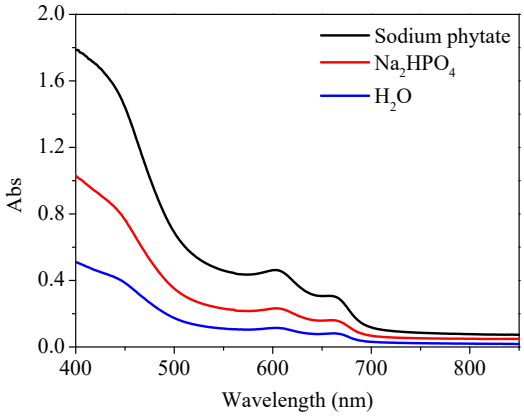

Figure S3. Absorption spectra of MoS_2 nanosheets obtained by ultrasonic exfoliation for 35 h in sodium phytate (1 mg·mL^{-1}), Na_2HPO_4 (3 mg·mL^{-1}) and water. The mass concentration of MoS_2 powder was 5 mg·mL^{-1}.

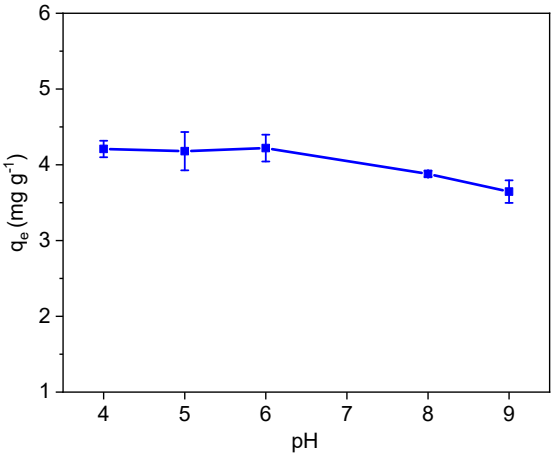

Figure S4. Effect of pH on the adsorption amount for Hg^{2+} by MoS_2 nanosheets exfoliated by sodium phytate. The mass of MoS_2 nanosheets was 6.4 mg. The initial concentration of Hg^{2+} was 1 μg·mL^{-1}. The adsorption equilibrium time was 1 h.

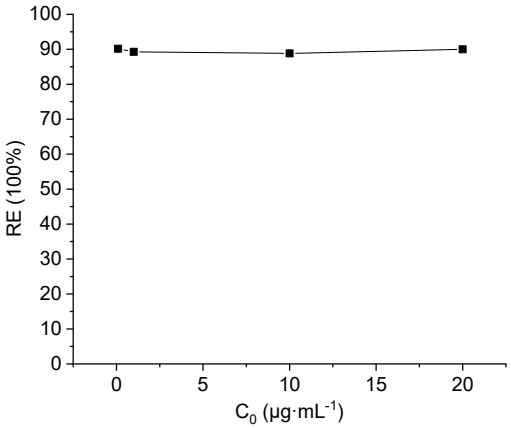

Figure S5. Effect of C_0 on the removal efficiency (RE) of MoS_2 nanosheets exfoliated by sodium phytate at 25°C.

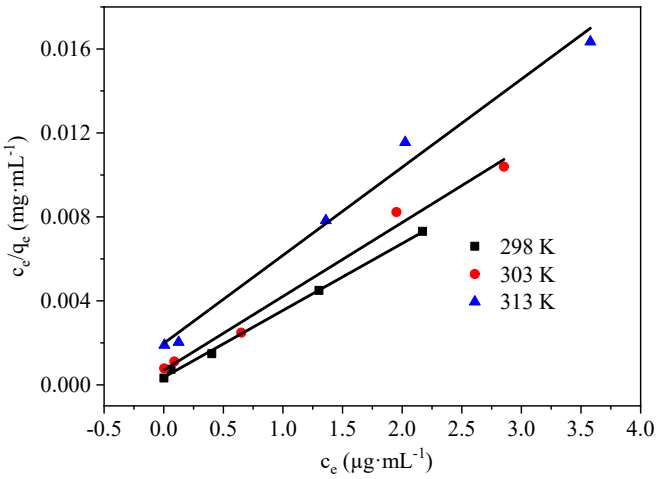

Figure S6. Langmuir adsorption isotherms of Hg^{2+} by MoS_2 nanosheets exfoliated by sodium phytate at different temperatures.

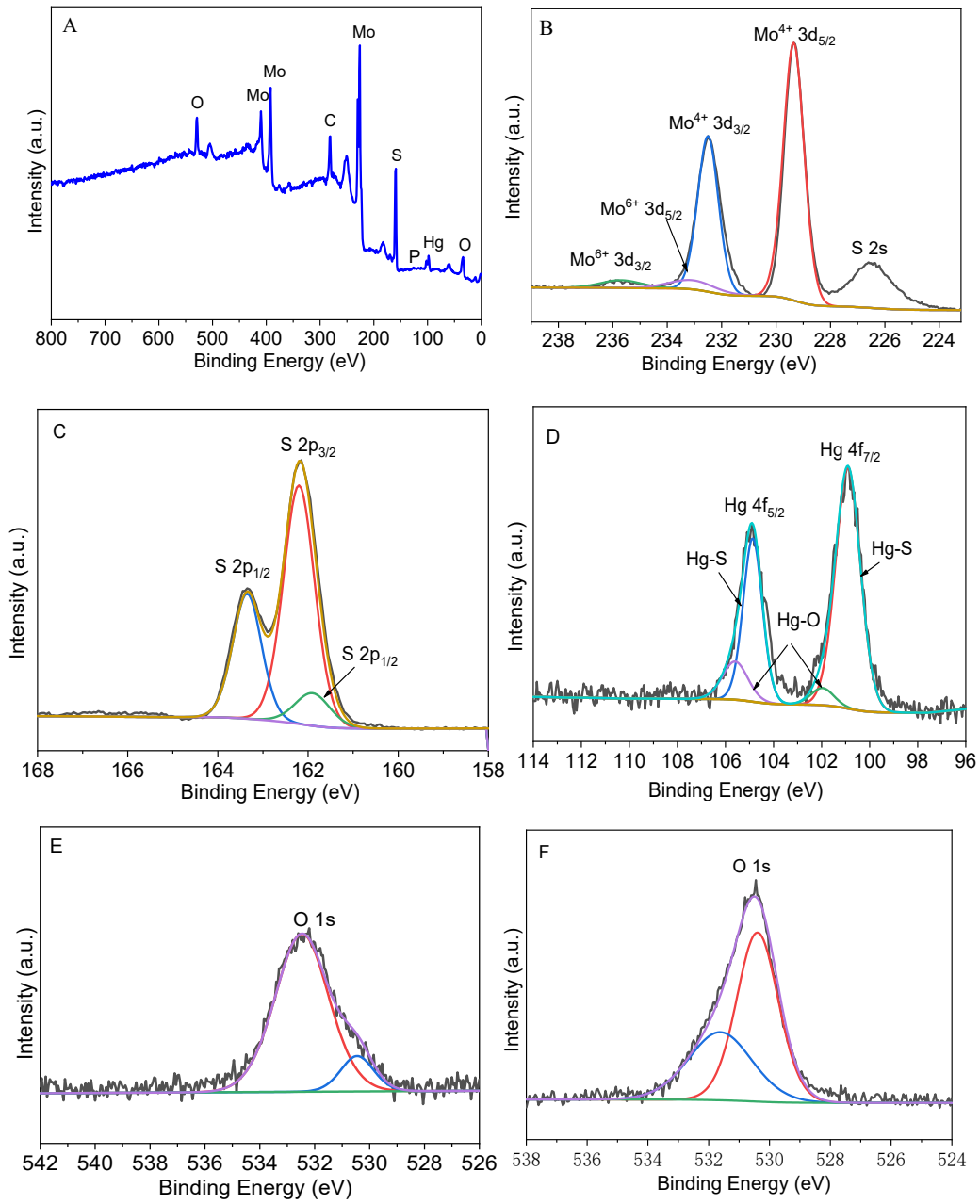

Figure S7. The survey (A), Mo 3d (B), S 2p (C), Hg 4f (E) and O 1s (E)core-level XPS spectra of MoS_2 nanosheets after Hg^{2+} adsorption, O 1s (F) core-level XPS spectra of MoS_2 nanosheets exfoliated by sodium phytate.

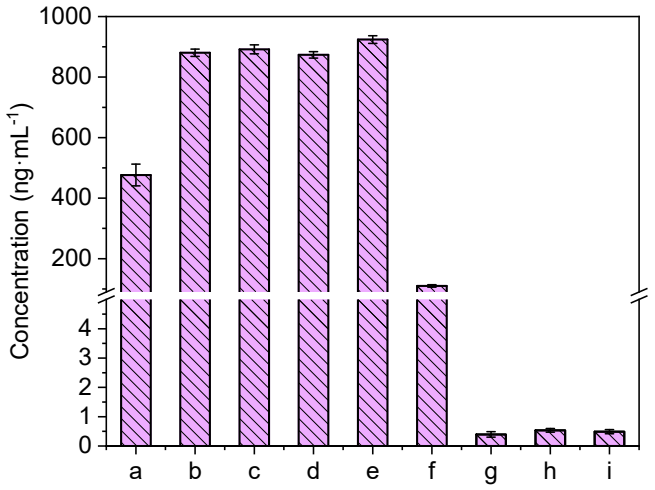

Figure S8. Concentration of residual metal ions after adsorption by MoS_2 nanosheets exfoliated by sodium phytate. (Concentrations of (a) Pb^{2+}, (b) Cd^{2+}, (c) Cr^{3+}, (d) Mn^{2+}, (e) Zn^{2+}, (f) Hg^{2+} were 1 μg·mL^{-1}, respectively; (g) Hg^{2+}: 100 ng·mL^{-1}; (h) Mixture 1: Hg^{2+}, Pb^{2+}, Cd^{2+}, Cr^{3+}, Mn^{2+}, Zn^{2+} are all 100 ng·mL^{-1}; (i) Mixture 2: Hg^{2+}, NO_2^-, NO_3^-, SO_4^{2-}, CO_3^{2-} are all 100 ng·mL^{-1}; MoS_2 nanosheets: 6.4 mg, adsorption time: 1 h).

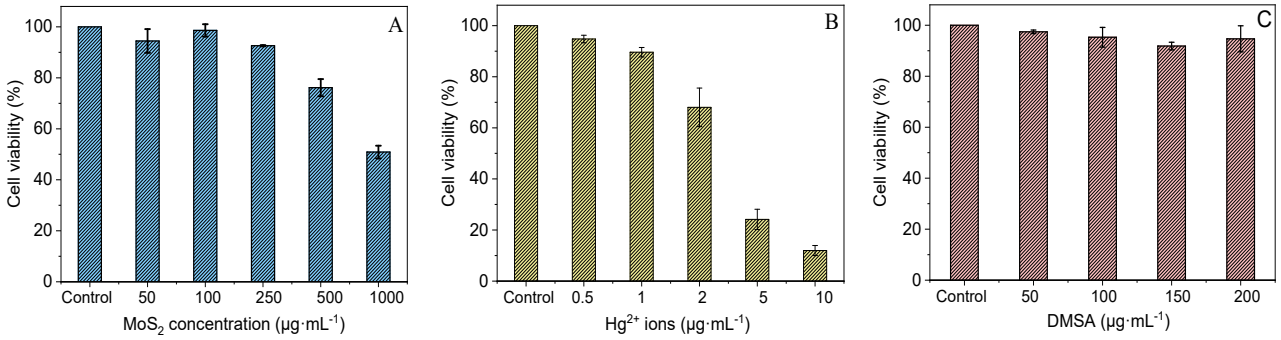

Figure S9. Viability of HepG2 cells after incubation in different concentrations of MoS_2 nanosheets exfoliated by sodium phytate (A), Hg^{2+} (B) and DMSA (C) for 12 h.

Table S1. Comparison of yields of MoS_2 nanosheets prepared by liquid ultrasonic exfoliation

Solvent/auxiliary reagent	Exfoliation time (h)	Yield	References
NMP	48 h	21%	[1]
ethyl alcohol/Water	8 h	0.6%	[2]
chloroform/acetonitrile	1 h	13.3%	[3]
alkali lignin	80 h	17.5%	[4]
TOCNs	4 h	18%	[5]
chitosan	5 h	25.5%	[6]
sodium cholate	16 h	10%	[7]
BSA	35 h	27.2%	[8]
tannin	2 h	60.5%	[9]
BSA-caged Au_{25} clusters	48	24%	[10]
ATP	30 h	23.6%	[11]
water	35 h	2.3%	This work
sodium phytate	35 h	18.1%	This work

Table S2. Adsorption dynamics model parameters

C_0 ($\mu g \cdot mL^{-1}$)	Pseudo-second order model		
	$q_{e,exp}$ ($mg \cdot g^{-1}$)	$q_{e,cal}$ ($mg \cdot g^{-1}$)	R^2
0.1	0.42	0.43	0.9992
1	4.19	4.22	0.9996
10	43.66	43.71	0.9969
20	85.30	86.73	0.9979

Table S3. The maximal adsorption capacity and correlation coefficient of Langmuir isotherms at different temperatures

Temperature	q_{max} ($mg \cdot g^{-1}$)	R^2
298 K	313.48	0.9976
303 K	284.09	0.9857
313 K	238.1	0.9842

Table S4. Comparison of the maximum adsorption capacity of MoS_2 for Hg^{2+}

Adsorbent	q_{max} ($mg \cdot g^{-1}$)	Reference
MoS_2 nanosheets exfoliated by sodium phytate	312.5 (25 °C)	This work
MoS_2 nanosheets exfoliated directly in water	85.47 (25 °C)	This work
MoS_2 powder	41.49 (25 °C)	This work
widened defect-rich nanoMoS_2 nanosheets	2563	[12]
2D MoS_2	254 (20 °C)/305 (35 °C)	[13]
Porous Au/Fe_3O_4/MoS_2CAs aerogel	1527	[14]
oxygen-incorporated MoS_2 nanosheets	1995.72	[15]
cellulose/MoS_2/Fe_3O_4 composite	469.48	[16]

References

1. J. Z. Huang, X. L. Deng, H. Wan, F. S. Chen, Y. F. Lin, X. J. Xu, R. Z. Ma and T. Sasaki, *ACS Sustain. Chem. Eng.,* 2018, **6**, 5227-5237.
2. K. G. Zhou, N. N. Mao, H. X. Wang, Y. Peng and H. L. Zhang, *Angew. Chem. Int. Ed.,* 2011, **50**, 10839-10842.
3. S. L. Zhang, H. Jung, J. S. Huh, J. B.Yu and W. C. Yang, *J. Nanosci. Nanotechnol.,* 2014, **14**, 8518-8522.

4. W. S. Liu, C. Y. Zhao, R. Zhou, D. Zhou, Z. L. Liu and X. H. Lu, *Nanoscale,* 2015, **7**, 9919-9926.
5. Y. Y. Li, H. L. Zhu, F. Shen, J. Y. Wan, S. Lacey, Z. Q. Fang, H. Q. Dai and L. B. Hu, *Nano Energy,* 2015, **13**, 346-354.
6. X. M. Feng, X. Wang, W. Y. Xing, K. Q. Zhou, L. Song and Y. Hu, *Compos. Sci. Technol.,* 2014, **93**, 76-82.
7. R. J. Smith, P. J. King, M. Lotya, C. Wirtz, U. Khan, S. De, A. Neill, G. S. Duesberg, J. C. Grunlan, G. Moriarty, J. Chen, J. Z. Wang, A. I. Minett, V. Nicolosi and J. N. Coleman, *Adv. Mater.,* 2011, **23**, 3944-3948.
8. G. J. Guan, S. Y. Zhang, S. Liu, Y. Q. Cai, M. Low, C. P. Teng, I. Y. Phang, Y. Cheng, K. L. Duei, B. M. Srinivasan, Y. Zhang, Y. W. Zhang and M. Y. Han, *J. Am. Chem. Soc.,* 2015, **137**, 6152-6155.
9. C. Zhang, D. F. Hu, J. W. Xu, M. Q. Ma, H. B. Xing, K. Yao, J. Ji and Z. K. Xu, *ACS Nano*, 2018, **12**, 12347-12356.
10. G. J. Guan, S. H. Liu, Y. Cheng, Y. W. Zhang and M. Y. Han, *Nanoscale*, 2018, **10**, 10911-10917.
11. X. L. Liu, H. Chen, J. Lin, Y. Li and L. Q. Guo, *Chem. Commun.*, 2019, **55**, 2972-2975.
12. K. Ai, C. P. Ruan, M. X. Shen and L. H. Lu, *Adv. Fun. Mater.,* 2016, **26**, 5542-5549.
13. F. F. Jia, Q. M. Wang, J. S. Wu, Y. M. Li and S. X. Song, *ACS Sustain. Chem. Eng.,* 2017, **5**, 7410-7419.
14. L. H. Zhi, W. Zuo, F. J. Chen and B. D. Wang, *ACS Sustain. Chem. Eng.,* 2016, **4**, 3398-3408.
15. W. Zhan, F. Jia, Y. Yuan, C. Liu, K. Sun, B. Yang and S. Song, and *J. Hazard. Mater.,* 2020, **384**, 121382.
16. P. Gao, J. Lei, J. Tan, G. Wang, H. Liu and L. Zhou, *Compos. Commun.,* 2021, **25**, 100736.